Article

High in vivo stability of 64Cu-labeled cross-bridged chelators is a crucial factor in improved tumor imaging of RGD peptide conjugates

Swarbhanu Sarkar, Nikunj Bhatt, Yeong su Ha, Phuong Tu Huynh, Nisarg Soni, Woong Hee Lee, Yong Jin Lee, Jung Young Kim, Darpan N. Pandya, Gwang Il An, Kyo Chul Lee, Yongmin Chang, and Jeongsoo Yoo

J. Med. Chem., **Just Accepted Manuscript** • DOI: 10.1021/acs.jmedchem.7b01671 • Publication Date (Web): 14 Dec 2017

High in vivo stability of ^{64}Cu-labeled cross-bridged chelators is a crucial factor in improved tumor imaging of RGD peptide conjugates

Swarbhanu Sarkar,[a,†] Nikunj Bhatt,[a,†] Yeong Su Ha,[a,†] Phuong Tu Huynh,[a] Nisarg Soni,[a] Woonghee Lee,[a] Yong Jin Lee,[b] Jung Young Kim,[b] Darpan N. Pandya,[a] Gwang Il An,[b] Kyo Chul Lee,[b] Yongmin Chang,[a] Jeongsoo Yoo [a,*]

[a]Department of Molecular Medicine, BK21 Plus KNU Biomedical Convergence Program, Kyungpook National University, Daegu 41944, South Korea. Fax: (+82) 53-426-4944.

[b]Molecular Imaging Research Center, Korea Institute of Radiological and Medical Sciences, Seoul 139-706, South Korea.

[†]Contributed equally to this work

Corresponding Author

* E-mail: yooj@knu.ac.kr. Phone: +82-53-420-4947. Fax: +82-53-426-4944

Abstract:

Although the importance of bifunctional chelators (BFCs) is well recognized, the chemophysical parameters of chelators that govern the biological behavior of the corresponding bioconjugates have not been clearly elucidated. Here, five BFCs closely related in structure were conjugated with a cyclic RGD peptide and radiolabeled with Cu-64 ions. Various biophysical and chemical properties of the Cu(II) complexes were analyzed with the aim of identifying correlations between individual factors and the biological behavior of the conjugates. Tumor uptake and body clearance of the ^{64}Cu-labeled bioconjugates were directly compared by animal PET imaging in animal models, which was further supported by biodistribution studies. Conjugates containing propylene cross-bridged chelators showed higher tumor uptake, while a closely related ethylene cross-bridged analog exhibited rapid body clearance. High in vivo stability of the copper-chelator complex was strongly correlated with high tumor uptake, while the overall lipophilicity of the bioconjugate affected both tumor uptake and body clearance.

Introduction

Radioactive copper is one of most actively studied radionuclides. It comprises several radioisotopes (^{60}Cu, ^{61}Cu, ^{62}Cu, ^{64}Cu or ^{67}Cu) having different decay modes, which are utilized for a wide range of applications from nuclear imaging to radiotherapy.[1-2] Among these, Cu-64 is most commonly used for the preparation of radiopharmaceuticals because of its attractive physical properties (β^+ 19%, β^- 38%, $t_{1/2}$ = 12.7 h) and good availability.[3-4] Some ^{64}Cu-labeled imaging probes are already used in humans and more are in clinical trials.[5] Recently, the use of radioactive copper for radiotherapy has gained more interest because of progress made in the production of the therapeutic nuclide Cu-67 (β^- 100%, $t_{1/2}$ = 61.8 h).[1, 6]

Even though several small copper complexes such as ^{64}Cu-ATSM and ^{64}Cu-PTSM have shown great potential as PET (positron emission tomography) imaging probes in the clinic,[7-8] most applications are as biomolecule conjugates, in which peptides or antibodies are radiolabeled with radioactive copper ions using bifunctional chelators (BFCs).[9-10] Ideally, BFCs will easily form robust copper complexes and should not lose copper ions under physiological conditions.[11-12] They also need to undergo straightforward conjugation with biomolecules, after which the intrinsic targeting properties of these compounds should not deteriorate.[13] For this, great efforts have been made worldwide to develop better chelators for copper ions.[10, 14-18] In particular, the observation that the widely employed chelator DOTA (1,4,7,10-tetraazacyclododecane-1,4,7,10-tetraacetic acid) loses copper ions in vivo accelerated the development of cross-bridged chelators that form ultrastable copper complexes. Initially, Wong and Anderson developed the cross-bridged chelator ECB-TE2A (ethylene cross-bridged 1,8-*N*,*N*′-bis-(carboxymethyl)-1,4,8,11-tetraazacyclotetradecane),[19] and recently propylene cross-bridged TE2A (PCB-TE2A) was added by our group.[20]

However, traditional BFCs such as DOTA, TETA, and DTPA derivatives are still most commonly chosen as chelators for the radiolabeling of biomolecules with Cu-64.[21-22] Although several studies have directly compared the effects of different chelators on radiolabeled bioconjugates, it remains unclear what properties of chelators are the most important determinants of the biological properties of bioconjugates, especially regarding tumor uptake, because of the small number of chelators compared and the non-systematic structural variations between them.[10, 23]

In this work, we carefully chose five BFCs with systematic variations in structure, focusing particularly on cross-bridged chelators. Five chelators were conjugated with the same RGD peptide and used for both in vitro and in vivo studies, including PET imaging. Various factors, including in vivo stability, lipophilicity, mode of conjugation, overall charge, linker, and specific activity, were directly compared and correlations between these parameters and tumor targeting efficacy were closely examined.

Results and discussion

Conjugation of BFCs with RGD peptides. Five BFCs were carefully selected for side-by-side comparison studies (Figure 1). Firstly, three cross-bridged chelators were selected. The original cross-bridged chelator, CB-TE2A, was directly compared with its propylene analog PCB-TE2A. Another PCB-TE2A derivative, PCB-TE2A-Bn-NCS, was also examined to assess the effect of the additional functionality on the chelator backbone. The non-cross-bridged chelator TE2A-Bn-NCS was chosen for direct comparison with cross-bridged PCB-TE2A-Bn-NCS. Finally, a NOTA derivative (NOTA-Bn-NCS), which is known to form a more stable copper complex than DOTA in vivo,[24] was compared with the others.

These chelators can be also categorized into two groups depending on their conjugation mode with biomolecules. Three chelators having an extra isothiocyanate group (-NCS) conjugate with cyclic RGDyK peptides (c(RGDyK)) via thiourea bonding, whereas ECB-TE2A and PCB-TE2A are linked to the peptide through amide bond formation using an acetate pendant arm (Figure 2). Specifically, NOTA-Bn-NCS and TE2A-Bn-NCS, the chelators bearing NCS functionality, were allowed to react with the free amine group on the lysine of the c(RGDyK) peptide in the presence of diisopropylethylamine (DIEA), and then purified by semi-preparative HPLC. The formation of the both bioconjugates was confirmed by ESI-MS. We used standard dicyclohexylcarbodiimide (DCC) coupling for the synthesis of PCB-TE2A-c(RGDyK) (**5**). In this protocol, the carboxylic group of PCB-TE2A was first activated by DCC/DIEA in dry DMSO, and the subsequent addition of the peptide allowed the amino group of lysine to react with the activated carboxylic acid group of PCB-TE2A; the bioconjugate was formed via an amide linkage. This compound was then purified and confirmed by ESI-MS, as described above for the NCS-bearing chelators. The other two bioconjugates, PCB-TE2A-Bn-NCS-c(RGDyK) (**3**) and ECB-TE2A-c(RGDyK) (**4**), were prepared according to the literature.[20, 25-26] The yields of the isolated conjugated products were 13%, 7%, and 9% for NOTA (**1**), TE2A (**2**), and PCB-TE2A (**5**), respectively.

Radiochemistry. Next, all bioconjugates were labeled with [^{64}Cu]$CuCl_2$ (37-370 MBq) at a concentration of 1 μg/20 μL (Figure 2), which was followed by HPLC purification to separate traces of free copper and minor impurities (Figure 3A–C, Supporting Information Figure S10). Although the radiochemical purity of all isolated ^{64}Cu-bioconjugates was determined to be > 95%, the radiolabeling conditions varied depending on the presence of cross-bridges on the chelators. For the non-cross-bridged chelates, NOTA (**1**) and TE2A (**2**), quantitative radiolabeling was

feasible at 50 °C within 15 min in simple water. However, the cross-bridged macrocycles, PCB-TE2A-Bn-NCS (**3**), ECB-TE2A (**4**), and PCB-TE2A (**5**), were radiolabeled at 80 °C in buffer (pH 8.0) with an extended incubation time of 60 min (Figure. 2). The radiolabeling yields of all three cross-bridged chelates were greater than 95%. Typical radiochemical yields were ~80% after HPLC purification from the start of radiolabeling. Total radiolabeling time including HPLC purification was less than 2 h.

The measured specific activities of all ^{64}Cu-bioconjugates was measured to be in the range of 15-40 GBq/μmol (Figure 3D). The cross-bridged chelates showed slightly higher specific activities than the non-cross-bridged chelates. Any meaningful correlation between specific activities and tumor uptakes was not observed.

Effect of BFCs on overall lipophilicity of bioconjugates. The LogD values at pH 7.4 of all radiolabeled bioconjugates are summarized in Figure 3D. As expected, the ECB-TE2A chelate (^{64}Cu-**4**), which conjugates amides directly with peptide via an acetate arm, showed the highest hydrophilicity (LogD -3.73). The PCB-TE2A chelate (^{64}Cu-**5**), which has an additional methylene bridging carbon compared with ECB-TE2A, had the next highest hydrophilicity (LogD -3.49). The overall charge of these two chelates after Cu(II) complexation is +1. The other three chelates, which contain an additional lipophilic benzyl isothiocyanate group (Bn-NCS), showed more lipophilic characteristics. Among these three chelates, NOTA-Bn-NCS (^{64}Cu-**1**), which has an overall charge of -1 after complexation, showed higher hydrophilicity (LogD -3.19), while PCB-TE2A-Bn-NCS (^{64}Cu-**3**), which contains a propylene cross-bridge and forms a neutral Cu(II) complex, was determined to be the most lipophilic (LogD -1.92). Another neutral complex, ^{64}Cu-TE2A-Bn-NCS-c(RGDyK) (^{64}Cu-**2**), showed much higher hydrophilicity than the PCB-TE2A-Bn-NCS conjugate (^{64}Cu-**3**) (LogD -3.38). Several factors, such as the overall charge of the copper

complex, the presence of an additional benzyl group, and the conjugation mode, thus seem to contribute to the overall lipophilic behavior of the peptide conjugates.[27]

Binding affinity assay. We then examined the $\alpha_v\beta_3$ integrin affinity of the five RGD conjugates (Figure 3E). Surface receptor binding assays, using $\alpha_v\beta_3$ integrin-positive U87MG cells and ^{125}I-echistatin as a radioligand, indicated that all bioconjugates selectively bind to the cell surface integrin receptor. The 50% inhibitory concentrations (IC_{50}) of the bioconjugates were all comparable and in the narrow range of 28–60 nM, which are similar to that of un-conjugated c(RGDyK) peptide itself (22.6 ± 4.77 nM). It is interesting to note that the direct conjugation of cross-bridged chelators with c(RGDyK) via an acetate group, resulted in minimal disturbance to its affinity towards $\alpha_v\beta_3$ integrin. It has been reported previously that the conjugation mode of the chelator has minimal impact on the integrin binding affinity of RGD conjugates.[25, 28-29] The ECB-TE2A (**4**) and PCB-TE2A (**5**) conjugates showed even lower IC_{50} values than the other three chelators with slightly long spacers between the chelator and the RGD moiety, although the differences were not large (Figure 3D).

In vitro and in vivo stability studies. First, we measured the serum stability of the ^{64}Cu-bioconjugates; no significant demetallation was observed for any chelator. For the least stable conjugate, the NOTA conjugate (^{64}Cu-**1**), 95% of the complex remained intact after 24 h incubation with fetal bovine serum at 37 °C, while the three cross-bridged chelators showed less than 1% decomplexation (Supporting Information Figure S1).

The plasma protein binding of ^{64}Cu-BFCs-c(RGDyK) was measured to be 17.5%, 12.9%, 12.5%, 15.8%, and 9.6% for NOTA (^{64}Cu-**1**), TE2A (^{64}Cu-**2**), PCB-TE2A-Bn-NCS (^{64}Cu-**3**), ECB-TE2A (^{64}Cu-**4**), and PCB-TE2A (^{64}Cu-**5**), respectively (Supporting Information Figure S2). No correlation between protein binding and stability or lipophilicity was observed.[30]

Next, we directly analyzed the in vivo stability of the ^{64}Cu-labeled bioconjugates in blood, liver, and kidney 1 h post-injection into Sprague-Dawley (SD) rats. In contrast to the in vitro serum stability data, there were large differences in in vivo stability between the different chelators (Fig. 4). In general, the three cross-bridged chelators showed much higher robustness compared with the two non-cross-bridged chelators. In particular, PCB-TE2A-Bn-NCS (^{64}Cu-**3**) showed exceptionally high stability in all three tissues. The blood demetallation of PCB-TE2A-Bn-NCS (^{64}Cu-**3**) was only 5.8%, whereas the blood demetallation of NOTA (^{64}Cu-**1**) and TE2A (^{64}Cu-**2**) was five times higher (30% and 40%, respectively), as determined by quantification of the demetalated free ^{64}Cu ion peak (Supporting Information Figure S3). The other cross-bridged chelators, which use one acetate group for peptide conjugation, showed intermediate inertness in blood (24% and 20% for ECB-TE2A (^{64}Cu-**4**) and PCB-TE2A (^{64}Cu-**5**), respectively). In liver, the stability differences between the cross-bridged and non-cross-bridged chelators were even more pronounced. All three cross-bridged chelators showed approximately 10% demetallation, which was only one quarter of that observed for the non-cross-bridged chelators (40% and 45% for NOTA (^{64}Cu-**1**) and TE2A (^{64}Cu-**2**), respectively). A very similar pattern was observed in the kidneys; demetallation was in the range of 8–12% for the cross-bridged chelators, whereas NOTA and TE2A showed approximately four-fold higher demetallation (34% and 45%, respectively). The ultrahigh robustness of PCB-TE2A-Bn-NCS can be explained by its tight clam shell-like holding of the copper ion with two acetate arms;[20] in contrast, the other two cross-bridged chelators use only one acetate arm for coordination to Cu(II) ions.

Animal PET imaging studies. A full comparative study to evaluate the in vivo behavior and tumor targeting efficacy of all ^{64}Cu-labeled bioconjugates was performed using animal PET imaging studies in U87MG tumor-bearing nude mice (n = 3 per bioconjugate). Representative

maximum intensity projection (MIP) PET images collected 1 h, 4 h, and 24 h post-injection are displayed in Figure 5. At first glance, most activity was found in clearance organs such as the liver, kidneys, intestine and bladder at 1 and 4 h post-injection (Figure 5A - J). After 24 h, most of the abdominal activity had been cleared from the body, and tumors became more easily distinguishable from the background for all five ^{64}Cu-bioconjugates (Figure 5K - O). However, upon closer inspection, all five conjugates showed distinct clearance and tumor uptake patterns. Tumors could be clearly identified from the background as early as 1 h post-injection in the case of the three cross-bridged chelators (Figure 5C–E), while the tumors could not be clearly identified until 24 h post-injection using the two non-cross-bridged chelators (Figure 5K & L). With respect to absolute tumor uptake, the two PCB-TE2A conjugates exhibited distinctively higher tumor uptake compared with the other three chelators (Figure 5C, H, M & 5E, J, O). The clearance patterns of the five conjugates were also different. The ECB-TE2A conjugate (^{64}Cu-**4**) exhibited the fastest body clearance via the urinary route,[31] while the two propylene cross-bridged chelators showed higher liver and kidney uptake at all time points compared with the other chelators. In particular, the PCB-TE2A-Bn-NCS bioconjugate (^{64}Cu-**3**) showed significant activity in the liver and intestine until 24 h post-injection (Figure 5M).

The detailed pharmacokinetic behavior of the ^{64}Cu-labeled conjugates was analyzed by PET image-based quantification. Regions of interest (ROIs) were drawn on liver, kidney, and muscle, as well as tumor tissue. The resulting quantitative data along with the tumor-to-organ ratios are summarized in Table 1. One of the strongest distinctions among the five ^{64}Cu-labeled peptides was the higher concentration of activity in tumors for two propylene cross-bridged chelators. The PCB-TE2A-Bn-NCS conjugate (^{64}Cu-**3**) exhibited the highest tumor uptakes at all time points (3.76 ± 0.21, 3.89 ± 0.07, 3.49 ± 0.10 %ID/g at 1, 4, 24 h, respectively), which was

followed by the PCB-TE2A conjugate (^{64}Cu-**5**) (3.45 ± 0.16, 3.10 ± 0.10, 2.34 ± 0.32 %ID/g). The ethylene cross-bridged chelator (^{64}Cu-**4**) showed the third highest tumor uptake until 4 h (2.23 ± 0.11, 1.99 ± 0.21 %ID/g at 1 and 4 h, respectively). In contrast to the non-cross-bridged chelators, which showed maximum uptake of less than 2 %ID/g in tumors at all time points, tumors could be visualized clearly using peptide conjugates of the three cross-bridged chelators. Even though the absolute tumor uptake of the ECB-TE2A conjugate (^{64}Cu-**4**) was lower than that of the PCB-TE2A conjugates (^{64}Cu-**5**), the tumors were more unambiguously visualized using the ECB-TE2A-conjugated peptide at 1 and 4 h because uptake of this conjugate in the neighboring liver and intestine was considerably lower than uptake of the other conjugates. Liver uptake of the ECB-TE2A conjugate (^{64}Cu-**4**) was less than half that of the PCB-TE2A-Bn-NCS conjugate (^{64}Cu-**3**) (1.97 ± 0.38 vs 3.91 ± 0.16 at 1 h, 1.66 ± 0.25 vs 3.15 ± 0.57 at 4 h, 0.79 ± 0.13 vs 2.73 ± 0.11 %ID/g at 24 h, respectively), resulting in the highest tumor-to-liver ratios at all time points (1.13, 1.20, 1.41 at 1, 4, and 24 h, respectively). In contrast to all other chelators, the ECB-TE2A conjugate (^{64}Cu-**4**) was rapidly excreted, mostly via the urinary route rather than the hepatobiliary route, which has also been observed by other groups.[25, 32] However, the PCB-TE2A conjugate (^{64}Cu-**5**), which has only one extra methylene carbon in the cross-bridge compared with the ECB-TE2A conjugate, resembled the PCB-TE2A-Bn-NCS conjugate (^{64}Cu-**3**) more closely than the ECB-TE2A conjugate in tumor uptake and clearance patterns. The PCB-TE2A conjugate (^{64}Cu-**5**) showed preferential excretion through the liver and intestine rather than the kidneys (3.91 ± 0.22 vs 2.97 ± 0.45 at 1 h, 3.13 ± 0.10 vs 2.25 ± 0.46 at 4 h, 1.83 ± 0.10 vs 1.60 ± 0.38 %ID/g at 24 h for liver and kidney, respectively). Considering that the chelators differ in their linker (the presence of the additional benzyl NCS group), the overall charge after Cu(II) complexation (neutral vs +1), and conjugation mode (thiourea vs amide), the closer resemblance of the PCB-

TE2A conjugate (^{64}Cu-**5**) to the PCB-TE2A-Bn-NCS conjugate (^{64}Cu-**3**) than the ECB-TE2A conjugate (^{64}Cu-**4**) is striking, and could be considered a good example of the importance of the bifunctional chelator in ^{64}Cu-labeled peptide conjugates.[25, 28] The only plausible explanation of this observation is that the high hydrophilicity of the ECB-TE2A conjugate (logD -3.73) facilitates urinary excretion.[33]

The improved tumor targeting efficacy—in terms of absolute tumor uptake and high tumor-to-background ratios—associated with the three cross-bridged chelators can be mostly attributed to the high in vivo stability of the corresponding Cu(II)-chelator complexes. As seen in Figure 4, the copper complexes of the three cross-bridged chelators showed much higher in vivo stability than the complexes of the non-cross-bridged chelators. Among the three cross-bridged chelators, ^{64}Cu-PCB-TE2A-Bn-NCS-c(RGDyK) (^{64}Cu-**3**), which exhibited the highest tumor uptake and prolonged tumor retention (Table 1), showed approximately four-fold lower demetallation in blood compared with the other two chelators. Ultrastable ^{64}Cu-labeled chelators could be delivered to the tumor region, minimizing the release of free ^{64}Cu(II) ions, which increases background activity and results in lower tumor-to-organ ratios.[25, 34] The lipophilicity of chelators also seems to have some effect on tumor uptake of ^{64}Cu-labeled bioconjugates.[35] Even though the in vivo stability of ^{64}Cu-PCB-TE2A-c(RGDyK) (^{64}Cu-**5**) was comparable with that of the ECB-TE2A analog (^{64}Cu-**4**), the PCB-TE2A conjugate, which had higher lipophilicity than the ECB-TE2A conjugate (LogD -3.49 vs -3.73), exhibited >1.5-fold higher tumor uptake at all three time points.

Biodistribution studies. Biodistribution studies of ^{64}Cu-TE2A-Bn-NCS-c(RGDyK) (^{64}Cu-**2**) and ^{64}Cu-PCB-TE2A-c(RGDyK) (^{64}Cu-**5**) were performed for the first time in the current study (Figure 6); biodistribution data for the other radiotracers have been reported previously.[20, 24, 32] Both of the ^{64}Cu-bioconjugates showed $\alpha_v\beta_3$ integrin-mediated specific tumor uptake. In

agreement with the PET imaging data, tumor uptake of ^{64}Cu-PCB-TE2A-c(RGDyK) (^{64}Cu-**5**) was two-fold higher than that of the TE2A-Bn-NCS conjugate (^{64}Cu-**2**) 1 h and 24 h post-injection (4.70 ± 0.35 vs 2.36 ± 0.41 at 1 h, 3.82 ± 0.23 vs 1.78 ± 0.04 %ID/g at 24 h). The PCB-TE2A conjugate (^{64}Cu-**5**) exhibited prolonged activity in tumors, and more than 80% of the activity observed 1 h post-injection remained after 24 h (Figure 6B). The activity in the other organs cleared gradually over time, resulting in high tumor-to-organ ratios at 24 h (22.6, 6.5, and 4.9 for blood, muscle, and liver, respectively). The relatively low tumor-to-kidney ratio of the PCB-TE2A conjugate (1.8) can be attributed to its preference for renal excretion, presumably because of its high hydrophilicity[25] (LogD −3.49) and the net positive charge of the tracer.[36-37] In contrast to the PCB-TE2A analog (^{64}Cu-**5**), the more lipophilic neutral ^{64}Cu-TE2A-Bn-NCS-c(RGDyK) conjugate (^{64}Cu-**2**) was excreted via both the liver and kidneys (Figure 6A), resulting in a lower tumor-to-liver ratio at all time points (0.71 vs. 2.1, 0.75 vs. 1.8, and 1.8 vs. 4.9, respectively). Prolonged retention in tumor and fast blood clearance also resulted in an increase in the tumor-to-blood ratio for ^{64}Cu-PCB-TE2A-c(RGDyK) (^{64}Cu-**5**) compared with ^{64}Cu-TE2A-Bn-NCS-c(RGDyK) (^{64}Cu-**2**) at all time points (6.8 vs. 4.4, 30.9 vs. 7.7, and 22.6 vs. 15.7 at 1, 4 and 24 h, respectively). In blocking studies, tumor uptake of TE2A-Bn-NCS (^{64}Cu-**2**) and PCB-TE2A (^{64}Cu-**5**) conjugates was reduced by 54% (1.09 ± 0.16 %ID/g) and 77% (1.08 ± 0.15 %ID/g), respectively, by co-injection of c(RGDyK) peptide, which clearly indicates that tumor uptake was mediated by specific binding of radiotracers to the $\alpha_v\beta_3$ integrin receptor (Figure 6A & B).

Conclusions

In the current study, the effects of bifunctional chelators on the pharmacokinetic behavior of ^{64}Cu-radiolabeled peptides were evaluated. Five closely related chelators, including three cross-

bridged macrocycles, were conjugated with cyclic RGD peptides and radiolabeled with Cu-64 ions in high yield. Various properties, such as in vitro and in vivo stability, LogD, specific activity, selective binding affinity, and protein binding, were measured. For biological evaluation, direct comparison of tumor uptake and body clearance among the five bioconjugates was achieved by animal PET imaging studies. Biodistribution studies further supported the imaging data.

Significant differences in tissue uptake and clearance patterns were observed depending on the chelator utilized in the peptide conjugate. The three cross-bridged chelators resulted in higher tumor visibility compared with the non-cross-bridged chelators. In particular, propylene cross-bridged chelators, which exhibited ultrahigh in vivo stability, showed higher tumor uptake, while the analogous ethylene cross-bridged chelator, which had the highest hydrophilicity, showed rapid body clearance. In our study, the in vivo stability of copper complexes was strongly correlated with tumor uptake of bioconjugates. Tumor targeting and body clearance, and therefore tumor-to-background ratios, also showed strong correlations with the overall lipophilicity of the ^{64}Cu-bioconjugates. No significant correlation between other factors (i.e., overall charge of the Cu(II) complex, linker, or conjugation mode of the chelator) and biological behavior was observed, although these factors might together contribute to the overall lipophilicity of the ^{64}Cu-bioconjugates. The effect of the chelator on the specific activity, selective binding affinity, and protein binding of the peptide conjugates was also minimal.

In conclusion, propylene cross-bridged TE2A derivatives show potential as promising bifunctional chelators for the radiolabeling of short peptides with radioactive copper ions, at least for RGD peptides. Further studies using PCB-TE2A chelators for radiolabeling of other disease-specific peptides for radioactive copper-based imaging and therapeutic applications are highly anticipated.

Experimental Section

Materials and methods. All chemicals or solvents used in the study were purchased from Sigma-Aldrich (St. Louis, USA) unless otherwise stated. c(RGDyK) was purchased from FutureChem (Seoul, Korea). Cu-64 was produced at KIRAMS (Seoul, Korea) by the $^{64}Ni(p,n)^{64}Cu$ nuclear reaction using an MC50 Cyclotron (Scanditronix, Sweden). All radio-TLC measurements were performed using a Bioscan 2000 imaging scanner (Bioscan, Washington, D.C., USA).

Conjugation of BFCs to c(RGDyK). The BFCs used in the study had two different functional groups (-NCS or -COOH), and two different coupling reactions were employed to conjugate the chelators to c(RGDyK) peptide depending on the functionality. For the synthesis of TE2A-Bn-NCS-c(RGDyK) (**2**), *N,N*-diisopropylethylamine (20 mmol) was added to a solution containing TE2A-Bn-NCS (10 μmol, 4.8 mg) and c(RGDyK) (10 μmol, 6.2 mg) in dimethylformamide (DMF; 1 mL), and the resulting mixture was stirred at room temperature for 16 h. A similar method was followed for the synthesis of NOTA-Bn-NCS-c(RGDyK) (**1**). Here NOTA-Bn-NCS (11 μmol, 5 mg) and c(RGDyK) (32 μmol, 10 mg) were used and the reaction was continued with *N,N*-diisopropylethylamine (40 mmol, 5 mg). Subsequently, the bioconjugates were purified by semi-preparative HPLC. HPLC conditions for TE2A-Bn-NCS-c(RGDyK) (**2**) and NOTA-Bn-NCS-c(RGDyK) (**1**) were as follows. For TE2A-Bn-NCS-c(RGDyK) (**2**), an Agilent preparative C18 column (5 μm, 21.2 × 100 mm) with the mobile phase (flow rate 3 mL/min) starting from 95% solvent A [0.1% TFA in water] and 5% solvent B [0.1% TFA in acetonitrile] [0–2 min] to 35% solvent A and 65% solvent B at 32 min was used. The peak containing the TE2A-Bn-NCS-c(RGDyK) (**2**) conjugate was collected at a retention time of 21.7 min, and it showed a retention

time of 12.8 min through analytical HPLC (Vydac TP C18, 3 μm, 4.6 × 100 mm; flow rate 1 mL/min, the mobile phase consisting of 0.1% TFA/H_2O (solvent A) and 0.1% TFA/acetonitrile (solvent B) with a gradient consisting of 1% B to 70% B in 20 min). For NOTA-Bn-NCS-c(RGDyK) (**1**), a Waters μbondapak C18 column (10 μm, 7.8 × 300 mm) with the mobile phase (flow rate 3 mL/min) starting from 95% solvent A (0.1% TFA in water) and 5% solvent B (0.1% TFA in acetonitrile) (0-2 min) to 35% solvent A and 65% solvent B at 32 min was used. The peak containing NOTA-Bn-NCS-c(RGDyK) conjugate (**1**) was collected at a retention time of 17.5 min. All fractions containing the product were combined and lyophilized to provide the final product as a white powder (isolated yield 7.3% and 13% for TE2A-Bn-NCS-c(RGDyK) (**2**) and NOTA-Bn-NCS-c(RGDyK) (**1**), respectively).

For the conjugation of PCB-TE2A to c(RGDyK), a typical amide coupling reaction was applied. *N,N′*-dicyclohexylcarbodiimides (10 mmol) and *N,N*-diisopropylethylamine (20 mmol) were added to a solution of PCB-TE2A (20 μmol, 7.2 mg) and c(RGDyK) (10 μmol, 6.2 mg) in DMSO (1 mL), and the reaction was allowed to continue at room temperature for 16 h. Finally, the pure PCB-TE2A-c(RGDyK) (**5**) was isolated as a white solid by HPLC purification [Zorbax Agilent Prep-C18; 21.2 × 100 mm; mobile phase starting from 95% solvent A (0.1% TFA in water) and 5% solvent B (0.1% TFA in acetonitrile) (0–2 min) to 35% solvent A and 65% solvent B at 32 min; flow rate 3 ml/min], which was followed by lyophilization (9.4% yield). Analytical HPLC identified the retention time of PCB-TE2A-c(RGDyK) (**5**) to be 12.2 min (Vydac TP C18, 3 μm, 4.6 x 100 mm; flow rate 1 mL/min, with the mobile phase consisting of 0.1% TFA/H_2O (solvent A) and 0.1% TFA/acetonitrile (solvent B) with a gradient consisting of 1% B to 70% B in 20 min). The other bioconjugates, ECB-TE2A-c(RGDyK) (**4**) and PCB-TE2A-Bn-NCS-c(RGDyK) (**3**) were prepared according to the published literature.[20, 26]

The formation of all bioconjugates was confirmed by ESI-MS. For TE2A-Bn-NCS-c(RGDyK), the calculated and identified m/z values for $C_{50}H_{76}N_{14}O_{12}S$ $[M+H]^+$ were 1097.56 and 1097.54 respectively (Supporting Information Figure S4). For NOTA-Bn-NCS-c(RGDyK) (**1**), the calculated and identified m/z values for $C_{47}H_{67}N_{13}O_{14}S$ $[M+H]^+$ were 1070.47 and 1070.5, respectively (Supporting Information Figure S5). For PCB-TE2A-c(RGDyK) (**5**), the calculated and identified m/z values for $C_{44}H_{71}N_{13}O_{11}$ $[M+H]^+$ were 958.5 and 958.2, respectively (Supporting Information Figure S6).

The chemical purities of the five isolated BFC-c(RGDyK) peptides were characterized by employing the second HPLC conditions. More than 95% chemical purity were obtained in all five peptide conjugates (Supporting Information Figure S9).

Radiolabeling with ^{64}Cu. Two different strategies were used for the radiolabeling of BFCs-c(RGDyK). For non-cross bridged macrocycles NOTA-Bn-NCS-c(RGDyK) (**1**) and TE2A-Bn-NCS-c(RGDyK) (**2**), $^{64}CuCl_2$ (18.5–148 MBq) in 100 μL MilliQ water (with no carrier added) was first mixed with 10 μg of BFCs-c(RGDyK) in 100 μL MilliQ water followed by incubation at 50 °C for 15 min using a ThermoMixer (800 rpm, Eppendorf). The radiolabeling progress was monitored by radio-TLC using Whatman MKC18F TLC plates developed with 10% NH_4OAc/methanol (3:7). Under this condition, ^{64}Cu-NOTA-Bn-NCS-c(RGDyK) (^{64}Cu-**1**) and ^{64}Cu-TE2A-Bn-NCS-c(RGDyK) (^{64}Cu-**2**) gave R_f values in the range of 0.9–1.0. For the cross bridged macrocycles, PCB-TE2A-Bn-NCS-c(RGDyK) (**3**), ECB-TE2A-c(RGDyK) (**4**), and PCB-TE2A-c(RGDyK) (**5**), the radiolabeling was performed in 0.1 M NH_4OAc buffer (pH 8.0) with an elongated incubation time of 60 min at 80 °C. Cross-bridged macrocycles gave R_f values of 0.8-0.9 under the same TLC condition. The ^{64}Cu-labeled peptide was then purified by reverse-phase

HPLC (RP-HPLC) using a Waters Grace smart RP C18 column (4.6 × 250 mm, 5 μm), with the mobile phase consisting of 0.1% TFA/H_2O or pure H_2O (solvent A, 0.1% TFA/H_2O and H_2O was used for cross-bridged and non-cross-bridged macrocycles, respectively) and 0.1% TFA/acetonitrile or acetonitrile (solvent B, 0.1% TFA/acetonitrile and acetonitrile was used for cross-bridged and non-cross-bridged macrocycles, respectively) and a gradient consisting of 1% B to 70% B in 20 min with a 1-mL/min flow rate. The radiotracers were collected in a fraction collector in 1–2 mL of HPLC eluent. The solvents were then evaporated at 37 °C and the activity was reconstituted in saline or 10% DMSO/saline, followed by passage through a 0.22-μm Millipore filter into a sterile dose vial for use in animal experiments. The radiochemical purities of ^{64}Cu-labeled NOTA-Bn-NCS (^{64}Cu-**1**), TE2A-Bn-NCS (^{64}Cu-**2**), PCB-TE2A-Bn-NCS (^{64}Cu-**3**), ECB-TE2A (^{64}Cu-**4**), and PCB-TE2A (^{64}Cu-**5**) bioconjugates after HPLC purification were 99%, 96%, 99%, 99%, and 95%, respectively (Figure 3A–C, Supporting Information Figure S7). The chemical purities for the same samples based on UV-HPLC chromatograms were 98.3%, 96.5%, 96.9%, 98.1%, and 97.7%, respectively.

Cold Cu(II)-BFCs-c(RGDyK) complexes were prepared by the reaction of BFCs-c(RGDyK) conjugates with 5 equivalent $CuCl_2$ in 0.1 M NH_4OAc (pH 8.0) buffer at 80 °C for 1 h, and used as internal standard for HPLC characterization without further purification. HRMS (FAB) for Cu-ECB-TE2A-c(RGDyK) (Cu-**4**). calcd. for $C_{43}H_{68}CuN_{13}O_{11}$ $[M]^+$ 1005.4457; found 1005.4460. HRMS (FAB) for Cu-PCB-TE2A-c(RGDyK) (Cu-**5**). calcd. for $C_{44}H_{70}CuN_{13}O_{11}$ $[M]^+$ 1019.4614; found 1019.4618.

In vitro serum stability. In vitro serum stability of all five radiotracers was performed by adding the ^{64}Cu-bioconjugate (50 μL, 7.4-13 MBq) to fetal bovine serum (500 μL). The mixture was then

incubated in a ThermoMixer (800 rpm) at 37 °C, and demetallation was analyzed by radio-TLC (10% NH_4OAc:MeOH = 3:7) at 0 h, 4 h, and 24 h.

Plasma protein binding assay. Plasma was prepared by centrifuging (10,000 rpm) blood (SD rat, male, 6 weeks) at 4 °C for 10 min just before the experiment. PD-10 columns (GE healthcare) were first preconditioned with 1 mL of 1% bovine serum albumin in 0.1 M DTPA, which was followed by repeated washing with saline (50 mL). ^{64}Cu-BFC-c(RGDyK) (0.55–0.75 MBq, 50 μL) was then incubated with plasma (1 mL) and PBS (1 mL) separately for 30 min at 37 °C. After the incubation, each sample was loaded on the preconditioned PD-10 column and eluted with saline; 30 fractions (500 μL each) were collected per sample in Eppendorf tubes. Radioactivity of each fraction was measured using a γ counter and a graph of radioactivity (CPM) vs saline volume (mL) was plotted.

Specific activity measurement. The specific activities of all the ^{64}Cu-bioconjugates were measured following previous reports.[20] Briefly, a calibration curve was first prepared by injecting various amounts (0–2 μg) of Cu-BFCs-c(RGDyK) into HPLC (λ_{max} = 220 nm). Non-radioactive Cu-complexes were prepared by incubating the BFCs-c(RGDyK) conjugates with excess $CuCl_2$ (10 mole equivalent) at 90 °C for 1 h. The pH of the reaction medium was maintained at 8 by adding NaOH solution (0.1 M). Subsequently, a known amount of activity of the purified ^{64}Cu-BFCs-c(RGDyK) (7.4–11.1 MBq) was injected into HPLC and the peak area obtained in the UV chromatogram was used to calculate specific activity (GBq/μmol).

Determination of partition coefficient. LogD values of all ^{64}Cu-bioconjugates were determined

by the octanol/PBS method. Briefly, 5 μL of the tracer (1.85 MBq) was added to a mixture of 1-octanol and phosphate buffered saline (pH 7.4) (1:1 v/v, 1 mL) and the resulting mixture was vortexed vigorously for 5 min at room temperature and centrifuged (10,000 rpm, 5 min) thereafter to ensure complete separation of both layers. Next, a 100-μL aliquot was taken from each phase and counted separately using a γ-counter. The partition coefficient was calculated as the ratio of counts in 1-octanol to that in PBS. The $LogD_{7.4}$ values were reported as an average of six measurements.

Integrin receptor binding assay. The cell-binding assay of the bioconjugates was performed using ^{125}I-echistatin on U87MG cells (2×10^6/100μL, resuspended in a binding buffer (20 mM tris, pH 7.4, 150 mM NaCl, 2 mM $CaCl_2$, 1 mM $MnCl_2$, and 0.1% bovine serum albumin) and IC_{50} values were compared to that of c(RGDyK). For this assay, equal volumes of all nonradioactive ligands, NOTA-Bn-NCS-c(RGDyK) (**1**), TE2A-Bn-NCS-c(RGDyK) (**2**), PCB-TE2A-Bn-NCS-c(RGDyK) (**3**), ECB-TE2A-c(RGDyK) (**4**), and PCB-TE2A-c(RGDyK) (**5**), and radioactive ^{125}I-echistatin (3.7 kBq, Perkin-Elmer, Branford, CT) were used. Various concentrations (10^{-5} to 10^{-14} M) of the ligands were incubated at room temperature for 60 min which was followed by the removal of the reaction medium. The cells were then washed with PBS (three times), harvested, and the bound ^{125}I-echistatin was counted in a γ-counter (1480 WIZARD, Wallac). Data were analyzed with GraphPad Prism 5 (GraphPad software, Inc., San Diego, CA) to calculate corresponding IC_{50} values. Each experiment was conducted in triplicate.

In vivo stability studies. In a typical experiment, approximately 37 MBq of radiolabeled conjugates was injected intravenously in SD rats (n = 2, male, 210 - 220 g). At 1 h post-injection,

the animals were sacrificed and blood and organs of interest (liver and kidney) were collected. To determine the stability of the bioconjugates in blood, the blood sample was immediately centrifuged (13,000 rpm for 10 min). Then, to the supernatant (200 μL), a solution mixture of acetonitrile/water/trifluoroacetic acid (50:45:5, 100 μL) was added. The mixture was then kept at 4 °C for 10 min and centrifuged again for 10 min at 13,000 rpm. The supernatant was then filtered through a 0.22-μm filter and injected into HPLC (Grace smart RP C18 column, 5 μm, 4.6 × 250 mm). The eluent [0.1% TFA/H_2O (solvent A) and 0.1% TFA/acetonitrile (solvent B), a gradient of 1% B to 70% B in 20 min at a flow rate of 1 mL/min] was collected with a fraction collector (1.0 min/fraction), and the radioactivity of each fraction was measured using a γ-counter. To determine the stability of ^{64}Cu-bioconjugates in the liver and kidney, the collected organs were first homogenized, which was followed by the addition of PBS (5 mL) and vigorous vortexing for 5 min. The mixture was then centrifuged for 10 min (13,000 rpm). To the supernatant (200 μL), 100 μL of a mixture of acetonitrile:water:trifluoroacetic acid (50:45:5) was added, which was followed by mixing and incubation at 4 °C for 10 min; samples were then centrifuged for 10 min at 13,000 rpm. The supernatant was then filtered through a 0.22-μm filter, and the filtrate was injected to reverse-phase HPLC; the activities of collected fractions were measured with a γ-counter. The in vivo stability of ^{64}Cu-NOTA-NCS-RGD (^{64}Cu-**1**), ^{64}Cu-TE2A-NCS-RGD (^{64}Cu-**2**), and ^{64}Cu-PCB-TE2A-RGD (^{64}Cu-**5**) were measured for the first time in the current manuscript, and the data were compared to that of ^{64}Cu-PCB-TE2A-Bn-NCS-RGD (^{64}Cu-**3**) and ^{64}Cu-ECB-TE2A-RGD (^{64}Cu-**4**), which were reported by us previously.[20]

The activities found in the precipitate from blood, liver and kidneys, were less than 10% and more than 90% of total tissue activities were used for the analysis.

Animal models. All the animal experiments were conducted in compliance with the guidelines set by the Institutional Animal Care and Use Committee requirements of Kyungpook National University. The procedures were reviewed and approved by the animal ethics committee of Kyungpook National University (Approval Number: 2016-0024). Specifically, 6-week old BALB/c female nude mice were used to prepare xenograft tumor models using U87MG cell lines. A total of 5×10^6 cells was inoculated subcutaneously into the right flank of the mice, and tumors of the appropriate size required approximately 15 days to develop.

Animal PET imaging. Small animal PET images were obtained using an Inveon PET-computed tomography (PET/CT) scanner (Siemens). All radiolabeled tracers (18.5–22.2 MBq, 200 μL 10% DMSO/saline) were injected via the tail vein into female nude mice bearing xenograft U87MG tumors on their right flank. At 1, 4, and 24 h post-injection, the mice were anesthetized with isoflurane (1–2 % in oxygen), positioned prone, and imaged using a PET scanner. CT images were acquired successively immediately after PET imaging without adding any additional contrast agent. All images were reconstructed using the 2-dimensional ordered-subsets expectation maximum (OSEM) algorithm. Regions of interest (ROIs) were manually drawn around the perimeters of the organs over 5-7 consecutive slices on transverse PET images entirely covering the most intense areas of ^{64}Cu-labelled BFC-c(RGDyK) uptake in the tumor, liver, kidney and muscle, while avoiding nearby tissues. Activity counts in the ROIs were calculated as the percentage of the injected dose per gram (%ID/g), and no corrections for attenuation were necessary. Since the location of ROIs on the PET images could not be accurately defined, we used the corresponding transverse CT images as a reference. The PET and CT volumes were manually co-registered for each of the scans (Inveon Research Workplace 4.0).

Biodistribution study. Under anesthesia using 1–2% isoflurane in O_2, tumor-bearing female BALB/c nude mice (n = 3 per group) were subjected to intravenous injection of the purified ^{64}Cu-bioconjugates (0.74 MBq, 200 µL saline) via tail vein. The animals were sacrificed at 1, 4, and 24 h post-injection and tissues of interest were explanted, weighted, and counted using a γ-counter (Wallac). Uptake in each tissue was expressed as percent of injected dose per gram (%ID/g) and was calculated by comparing the samples with a standard solution derived from the injected solution. For the blocking study, non-radioactive c(RGDyK) was co-injected (5 mg/kg) with ^{64}Cu-labelled tracers in tumor models and biodistribution was conducted 1 h post-injection.

ASSOCIATED CONTENT

Supporting Information

The Supporting Information is available free of charge on the ACS Publications website at DOI:

Serum stability studies of ^{64}Cu-BFCs-c(RGDyK), plasma protein binding studies of ^{64}Cu-BFCs-c(RGDyK), in vivo stability studies of ^{64}Cu-BFCs-c(RGDyK), mass spectra of BFCs-c(RGDyK) conjugates, UV HPLC profiles of BFCs-c(RGDyK) conjugates, UV/radio-HPLC chromatogram of ^{64}Cu-PCB-TE2A-Bn-NCS-c(RGDyK) and ^{64}Cu-ECB-TE2A-c(RGDyK), mass spectra of Cu-ECB-TE2A-c(RGDyK) and Cu-PCB-TE2A-c(RGDyK).

AUTHOR INFORMATION

Corresponding Author

*J.Y.: phone, +82-53-420-4947; e-mail, yooj@knu.ac.kr.

ORCID

Jeongsoo Yoo: 0000-0002-0752-5745

Author Contributions

S.S, N.B and Y.S.H contributed equally to this work.

ACKNOWLEDGMENTS

This work was supported by an R&D program through the National Research Foundation of Korea funded by the Ministry of Science, ICT & Future Planning (No. 2016R1A2B4011546, 2013R1A4A1069507, 2017M2C2A1014006, 2017M2A2A6A02018506, and 2016H1D3A1907667) and supported by a grant of the Korea Health Technology R&D Project through the Korea Health Industry Development Institute (KHIDI), funded by the Ministry of Health & Welfare, Republic of Korea (grant number: HI17C0221).

ABBREVIATIONS USED

BFCs, bifunctional chelators; RGD, arginylglycylaspartic acid; PET, positron-emission tomography; ATSM, diacetyl-bis(N4-methylthiosemicarbazone); PTSM, pyruvaldehyde bis(N4-methylthiosemicarbazone); DOTA, 1,4,7,10-tetraazacyclododecane-1,4,7,10-tetraacetic acid; ECB-TE2A, ethylene cross-bridged 1,8-*N*,*N*′-bis-(carboxymethyl)-1,4,8,11-tetraazacyclotetradecane; PCB-TE2A, propylene cross-bridged 1,8-*N*,*N*′-bis-(carboxymethyl)-1,4,8,11-tetraazacyclotetradecane; TETA, 1,4,8,11-tetraazacyclotetradecane-*N*,*N*',*N*'',*N*'''-tetraacetic acid; DTPA, diethylenetriaminepentaacetic acid; PCB-TE2A-Bn-NCS, 4,11-*N*,*N*′-bis(carboxymethyl)-16-(4-isothiocyanatobenzyl)-1,4,8,11-tetraazabicyclo[6.6.3]heptadecane; TE2A-Bn-NCS, 1,8-*N*,*N*′-bis-(carboxymethyl)-4-*N*″-(4′-isothiocyanatophenethyl)-1,4,8,11-tetraazacyclotetradecane; NOTA, 1,4,7-triazacyclododecane-*N*,*N*′,*N*″-triacetic acid); NOTA-Bn-NCS, 2-S-(4-isothiocyanatobenzyl)-1,4,7-triazacyclononane-1,4,7-triacetic acid; HPLC, high performance liquid chromatography; DIEA, *N*,*N*-diisopropylethylamine; ESI-MS, electrospray ionization mass spectrometry; HRMS, high resolution mass spectrometry; FAB, fast atom bombardment; DCC, dicyclohexylcarbodiimides; DMSO, dimethylsulfoxide; IC, inhibitory concentrations; SD rat, Sprague-Dawley rat; MIP, maximum intensity projection; TLC, thin layer chromatography; rpm, revolutions per minute; DMF, dimethylformamide; TFA, trifluoroacetic acid ; %ID/g, percent injected dose per gram; CPM, counts per minute; PBS, phosphate buffered saline; ROI, region of interest; CT, computed tomography.

References

(1) Blower, P. J.; Lewis, J. S.; Zweit, J. Copper radionuclides and radiopharmaceuticals in nuclear medicine. *Nucl. Med. Biol.* **1996**, *23*, 957-980.

(2) Donnelly, P. S. The role of coordination chemistry in the development of target-specific radiopharmaceuticals. *Dalton Trans.* **2011**, *40*, 999-1010.

(3) Kume, M.; Carey, P. C.; Gaehle, G.; Madrid, E.; Voller, T.; Margenau, W.; Welch, M. J.; Lapi, S. E. A semi-automated system for the routine production of copper-64. *Appl. Radiat. Isot.* **2012**, *70*, 1803-1806.

(4) Shokeen, M.; Anderson, C. J. Molecular imaging of cancer with copper-64 radiopharmaceuticals and positron emission tomography (PET). *Acc. Chem. Res.* **2009**, *42*, 832-841.

(5) Anderson, C. J.; Ferdani, R. Copper-64 radiopharmaceuticals for PET imaging of cancer: advances in preclinical and clinical research. *Cancer Biother. Radiopharm*. **2009**, *24*, 379-393.

(6) Novak-Hofer, I.; Schubiger, P. A. Copper-67 as a therapeutic nuclide for radioimmunotherapy. *Eur. J. Nucl. Med. Mol. Imaging* **2002**, *29*, 821.

(7) Dehdashti, F.; Grigsby, P. W.; Mintun, M. A.; Lewis, J. S.; Siegel, B. A.; Welch, M. J. Assessing tumor hypoxia in cervical cancer by positron emission tomography with ^{60}Cu-ATSM: relationship to therapeutic response-a preliminary report. *Int. J. Radiat. Oncol. Biol. Phys.* **2003**, *55*, 1233-1238.

(8) Colombie, M.; Gouard, S.; Frindel, M.; Vidal, A.; Cherel, M.; Rousseau, C.; Kraeber-Bodere, F.; Bourgeois, M. Focus on the controversial aspects of ^{64}Cu-ATSM in tumoral hypoxia mapping by PET imaging. *Front. Med.* **2015**, *2*, 1-7.

(9) Fani, M.; Del, P. L.; Abiraj, K.; Mansi, R.; Tamma, M. L.; Cescato, R.; Waser, B.; Weber, W. A.; Reubi, J. C.; Maecke, H. R. PET of somatostatin receptor-positive tumors using ^{64}Cu- and ^{68}Ga-somatostatin antagonists: the chelate makes the difference. *J. Nucl. Med.* **2011**, *52*, 1110-1118.

(10) Cooper, M. S.; Ma, M. T.; Sunassee, K.; Shaw, K. P.; Williams, J. D.; Paul, R. L.; Donnelly, P. S.; Blower, P. J. Comparison of ^{64}Cu-complexing bifunctional chelators for radioimmunoconjugation: labeling efficiency, specific activity, and in vitro/in vivo stability. *Bioconjugate Chem.* **2012,** *23*, 1029-1039.

(11) Bartholomä, M. D. Recent developments in the design of bifunctional chelators for metal-based radiopharmaceuticals used in positron emission tomography. *Inorg. Chim. Acta.* **2012,** *389*, 36-51.

(12) Zeglis, B. M.; Lewis, J. S. A practical guide to the construction of radiometallated bioconjugates for positron emission tomography. *Dalton Trans.* **2011,** *40*, 6168-6195.

(13) Liu, S. Bifunctional coupling agents for radiolabeling of biomolecules and target-specific delevery of metallic radionuclides. *Adv. Drug Deliver. Rev.* **2008**, *60*, 1347-1370.

(14) Gai, Y.; Sun, L.; Hui, W.; Ouyang, Q.; Anderson, C. J.; Xiang, G.; Ma, X.; Zeng, D. New Bifunctional chelator p-SCN-PhPr-NE3TA for copper-64: synthesis, peptidomimetic conjugation, radiolabeling, and evaluation for PET imaging. *Inorg. Chem.* **2016**, *55*, 6892-6901.

(15) Pandya, D. N.; Kim, J. Y.; Park, J. C.; Lee, H.; Phapale, P. B.; Kwak, W.; Choi, T. H.; Cheon, G. J.; Yoon, Y.-R.; Yoo, J. Revival of TE2A; a better chelate for Cu(II) ions than TETA? *Chem. Commun.* **2010**, *46*, 3517-3519.

(16) Sprague, J. E.; Peng, Y.; Sun, X.; Weisman, G. R.; Wong, E. H.; Achilefu, S.; Anderson, C. J. Preparation and biological evaluation of copper-64-labeled tyr3-octreotate using a cross-bridged

macrocyclic chelator. *Clin. Cancer Res.* **2004**, *10*, 8674-8682.

(17) Singh, A. N.; Dakanali, M.; Hao, G.; Ramezani, S.; Kumar, A.; Sun, X. Enantiopure bifunctional chelators for copper radiopharmaceuticals - does chirality matter in radiotracer design? *Eur. J. Med. Chem.* **2014**, *80*, 308-315.

(18) Chong, H.-S.; Ma, X.; Le, T.; Kwamena, B.; Milenic, D. E.; Brady, E. D.; Song, H. A.; Brechbiel, M. W. Rational design and generation of a bimodal bifunctional ligand for antibody-targeted radiation cancer therapy. *J. Med. Chem*. **2007**, *51*, 118-125.

(19) Wong, E. H.; Weisman, G. R.; Hill, D. C.; Reed, D. P.; Rogers, M. E.; Condon, J. S.; Fagan, M. A.; Calabrese, J. C.; Lam, K.-C.; Guzei, I. A.; Rheingold, A. L. Synthesis and characterization of cross-bridged cyclams and pendant-armed derivatives and structural studies of their copper(II) complexes. *J. Am. Chem. Soc.* **2000**, *122*, 10561-10572.

(20) Pandya, D. N.; Bhatt, N.; An, G. I.; Ha, Y. S.; Soni, N.; Lee, H.; Lee, Y. J.; Kim, J. Y.; Lee, W.; Ahn, H. Propylene cross-bridged macrocyclic bifunctional chelator: a new design for facile bioconjugation and robust ^{64}Cu complex stability. *J. Med. Chem.* **2014,** *57*, 7234-7243.

(21) Lewis, M. R.; Boswell, C. A.; Laforest, R.; Buettner, T. L.; Ye, D.; Connett, J. M.; Anderson, C. J. Conjugation of monoclonal antibodies with TETA using activated esters: biological comparison of ^{64}Cu-TETA-1A3 with ^{64}Cu-BAT-2IT-1A3. *Cancer Biother. Radiopharm.* **2001**, *16*, 483-494.

(22) Lewis, M. R.; Kao, J. Y.; Anderson, A. L.; Shively, J. E.; Raubitschek, A. An improved method for conjugating monoclonal antibodies with N-hydroxysulfosuccinimidyl DOTA. *Bioconjugate Chem.* **2001**, *12*, 320-324.

(23) Litau, S.; Seibold, U.; Vall-Sagarra, A.; Fricker, G.; Wängler, B.; Wängler, C. Comparative assessment of complex stabilities of radiocopper chelating agents by a combination of complex

challenge and in vivo experiments. *ChemMedChem* **2015,** *10*, 1200-1208.

(24) Liu, Z.; Li, Z.-B.; Cao, Q.; Liu, S.; Wang, F.; Chen, X. Small-animal PET of tumors with ^{64}Cu-labeled RGD-bombesin heterodimer. *J. Nucl. Med.* **2009,** *50*, 1168-1177.

(25) Wei, L.; Ye, Y.; Wadas, T. J.; Lewis, J. S.; Welch, M. J.; Achilefu, S.; Anderson, C. J. ^{64}Cu-Labeled CB-TE2A and diamsar-conjugated RGD peptide analogs for targeting angiogenesis: comparison of their biological activity. *Nucl. Med. Biol.* **2009,** *36*, 277-285.

(26) Sprague, J. E.; Kitaura, H.; Zou, W.; Ye, Y.; Achilefu, S.; Weilbaecher, K. N.; Teitelbaum, S. L.; Anderson, C. J. Noninvasive imaging of osteoclasts in parathyroid hormone-induced osteolysis using a ^{64}Cu-labeled RGD peptide. *J. Nucl. Med.* **2007**, *48*, 311-318.

(27) Van de Waterbeemd, H.; El Tayar, N.; Carrupt, P. A.; Testa, B. Pattern recognition study of QSAR substituent descriptors. *J. Comput. Aid. Mol. Des.* **1989**, *3*, 111-132.

(28) Wu, Y.; Zhang, X.; Xiong, Z.; Cheng, Z.; Fisher, D. R.; Liu, S.; Gambhir, S. S.; Chen, X. microPET Imaging of glioma integrin $\alpha_v\beta_3$ expression using ^{64}Cu-labeled tetrameric RGD peptide. *J. Nucl. Med.* **2005**, *46*, 1707-1718.

(29) Yoo, J. S.; Lee, J.; Jung, J. H.; Moon, B. S.; Kim, S.; Lee, B. C.; Kim, S. E. SPECT/CT imaging of high-risk atherosclerotic plaques using integrin-binding RGD dimer peptides. *Sci. Rep*. **2015**, *5*, 11752-11763.

(30) Smith, D. A.; Di, L.; Kerns, E. H., The effect of plasma protein binding on in vivo efficacy: misconceptions in drug discovery. *Nat. Rev. Drug Discovery* **2010,** *9* (12), 929-939.

(31) Banerjee, S. R.; Pullambhatla, M.; Foss, C. A.; Nimmagadda, S.; Ferdani, R.; Anderson, C. J.; Mease, R. C.; Pomper, M. G., ^{64}Cu-Labeled inhibitors of prostate-specific membrane antigen for PET imaging of prostate cancer. *J. Med. Chem.* **2014,** *57* (6), 2657-2669.

(32) Dumont, R. A.; Deininger, F.; Haubner, R.; Maecke, H. R.; Weber, W. A.; Fani, M. Novel ^{64}Cu-and ^{68}Ga-labeled RGD conjugates show improved PET imaging of $\alpha_v\beta_3$ integrin expression and facile radiosynthesis. *J. Nucl. Med.* **2011,** *52*, 1276-1284.

(33) Waring, M. J. Lipophilicity in drug discovery. *Expert Opin. Drug Discovery* **2010**, *5*, 235-248.

(34) Boswell, C. A.; Sun, X.; Niu, W.; Weisman, G. R.; Wong, E. H.; Rheingold, A. L.; Anderson, C. J. Comparative in vivo stability of copper-64-labeled cross-bridged and conventional tetraazamacrocyclic complexes. *J. Med. Chem.* **2004,** *47*, 1465-1474.

(35) Wang, J.; Yang, C.-T.; Kim, Y.-S.; Sreerama, S. G.; Cao, Q.; Li, Z.-B.; He, Z.; Chen, X.; Liu, S. ^{64}Cu-Labeled triphenylphosphonium and triphenylarsonium cations as highly tumor-selective imaging agents. *J. Med. Chem.* **2007**, *50*, 5057-5069.

(36) Rogers, B. E.; Anderson, C. J.; Connett, J. M.; Guo, L. W.; Edwards, W. B.; Sherman, E. L.; Zinn, K. R.; Welch, M. J. Comparison of four bifunctional chelates for radiolabeling monoclonal antibodies with copper radioisotopes: biodistribution and metabolism. *Bioconjugate Chem.* **1996,** 7, 511-522.

(37) Yoo, J.; Reichert, D. E.; Welch, M. J. Comparative in vivo behavior studies of cyclen-based copper-64 complexes: regioselective synthesis, X-ray structure, radiochemistry, log P, and biodistribution. *J. Med. Chem.* **2004,** *47*, 6625-6637.

Figure Captions

Figure 1. Structures of BFC-c(RGDyK) conjugates, NOTA-Bn-NCS-c(RGDyK) (**1**), TE2A-Bn-NCS-c(RGDyK) (**2**), PCB-TE2A-Bn-NCS-c(RGDyK) (**3**), ECB-TE2A-c(RGDyK) (**4**), and PCB-TE2A-c(RGDyK) (**5**).

Figure 2. Synthetic procedures for the ^{64}Cu-bioconjugates. A) Conjugation strategies for non-cross bridged chelators, TE2A-Bn-NCS and NOTA-Bn-NCS, to c(RGDyK), and radiolabeling with Cu-64. B) Conjugation of PCB-TE2A to c(RGDyK) and radiolabeling with Cu-64. Reaction conditions: (i) diisopropylethylamine (DIEA), dimethylformamide (DMF), room temperature, 16 h; (ii) $^{64}CuCl_2$, water, 50 °C, 15 min; (iii) dicyclohexylcarbodiimide (DCC), DIEA, DMSO, room temperature, 16 h; (iv) $^{64}CuCl_2$, 0.1 M NH_4OAc buffer (pH 8), 80 °C, 60 min.

Figure 3. (A–C) UV-HPLC (230 nm, black) and radio-HPLC (red) chromatogram of bioconjugates. A) UV/radio HPLC chromatogram of ^{64}Cu-NOTA-Bn-NCS-c(RGDyK) (^{64}Cu-**1**). B) UV/radio HPLC chromatogram of ^{64}Cu-TE2A-Bn-NCS-c(RGDyK) (^{64}Cu-**2**). C) UV/radio HPLC chromatogram of ^{64}Cu-PCB-TE2A-c(RGDyK) (^{64}Cu-**5**). D) Measurement of the biophysical properties of the bioconjugates. E) In vitro inhibition of ^{125}I-echistain binding to integrin on U87MG cells by c(RGDyK) and bioconjugates.

Figure 4. In vivo stability of radiotracers in rat tissues at 1 h post-injection.

Figure 5. Representative PET (A–J) and PET/CT (K–O) images of bioconjugates in U87MG tumor-bearing mice at 1, 4, and 24 h post-injection (n = 3 for each group). PET images are shown in maximum intensity projection mode. All images are decay-corrected and adjusted to the same maximum value. (A, F, K) ^{64}Cu-NOTA-Bn-NCS-c(RGDyK) (^{64}Cu-**1**), (B, G, L) ^{64}Cu-TE2A-Bn-NCS-c(RGDyK) (^{64}Cu-**2**), (C, H, M) ^{64}Cu-PCB-TE2A-Bn-NCS-c(RGDyK) (^{64}Cu-**3**), (D, I, N) ^{64}Cu-ECB-TE2A-c(RGDyK) (^{64}Cu-**4**), and (E, J, O) ^{64}Cu-PCB-TE2A-c(RGDyK) (^{64}Cu-**5**). White arrowhead indicates tumor.

Figure 6. Biodistribution data of (A) ^{64}Cu-TE2A-Bn-NCS-c(RGDyK) (^{64}Cu-**2**) and (B) ^{64}Cu-PCB-TE2A-c(RGDyK) (^{64}Cu-**5**) at 1 h, 1 h with blocking, and 4 and 24 h post-injection in U87MG tumor-bearing nude mice (n = 3).

Table 1. Tumor, liver, kidney, and muscle uptakes of ^{64}Cu-bioconjugates at 1 h (A), 4 h (B), and 24 h (C) post-injection. Organ uptakes are presented as %ID/g. Quantification was calculated based on the PET/CT images depicted in Figure 5.

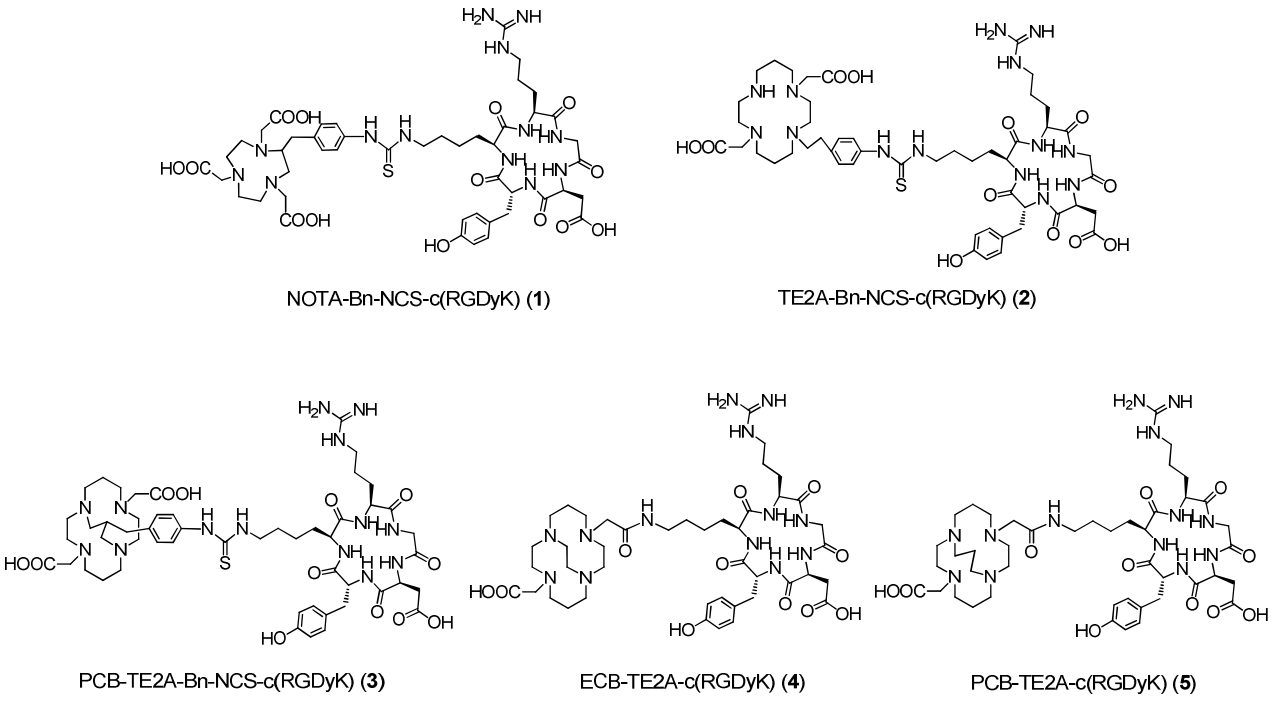
NOTA-Bn-NCS-c(RGDyK) (1)
TE2A-Bn-NCS-c(RGDyK) (2)
PCB-TE2A-Bn-NCS-c(RGDyK) (3)
ECB-TE2A-c(RGDyK) (4)
PCB-TE2A-c(RGDyK) (5)

Figure 1.

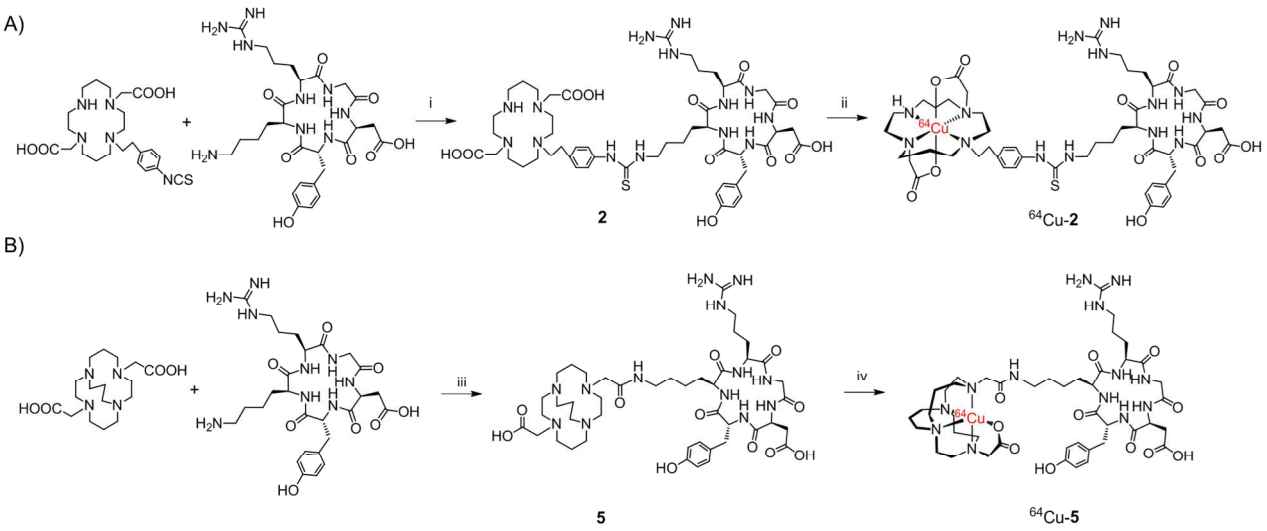

Figure 2.

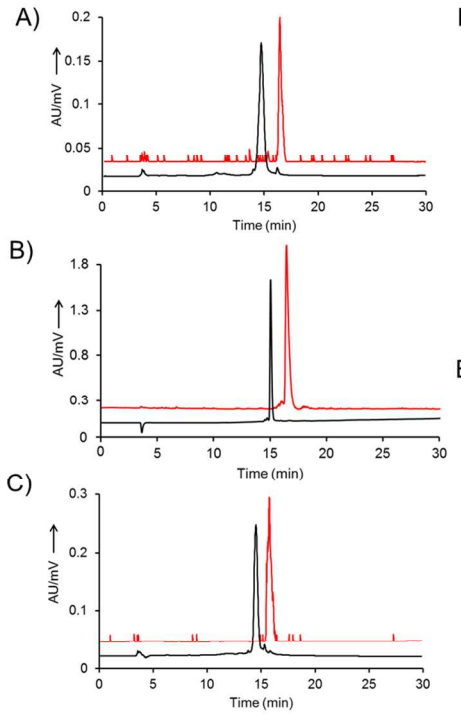

D)

Bioconjugates	Specific activity (GBq/μmol)	$LogD_{7.4}$	IC_{50} (nM)
c(RGDyK)	-	-	22.60 ± 4.77
^{64}Cu-NOTA-Bn-NCS-c(RGDyK)	15.9	-3.19	51.96 ± 3.59
^{64}Cu-TE2A-Bn-NCS-c(RGDyK)	19.2	-3.38	59.30 ± 5.95
^{64}Cu-PCB-TE2A-Bn-NCS-c(RGDyK)	39.7	-1.92	60.50 ± 11.81
^{64}Cu-ECB-TE2A-c(RGDyK)	34.9	-3.73	46.60 ± 20.35
^{64}Cu-PCB-TE2A-c(RGDyK)	26.3	-3.49	28.22 ± 8.63

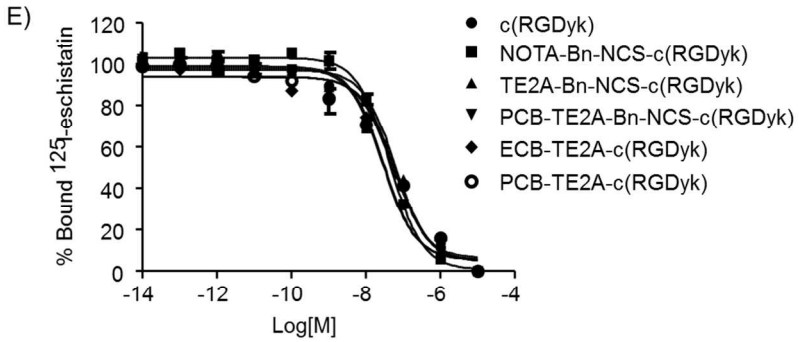

Figure 3.

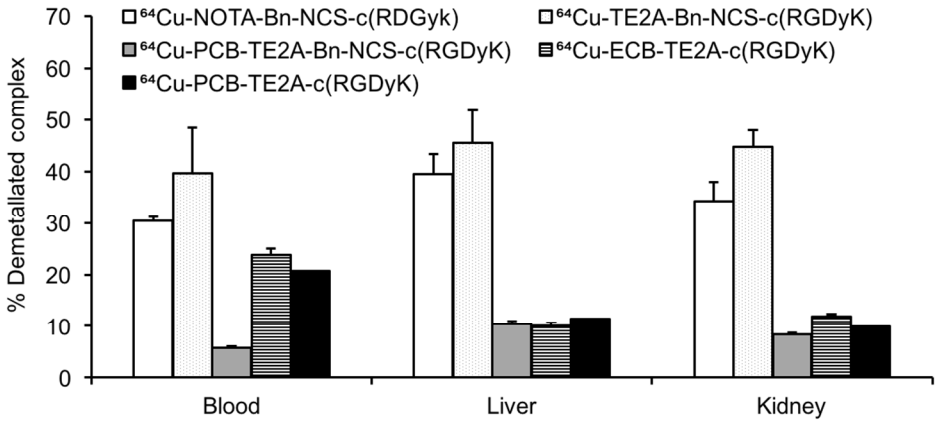
% Demetallated complex
70
60
50
40
30
20
10
0
64Cu-NOTA-Bn-NCS-c(RDGyk)
64Cu-TE2A-Bn-NCS-c(RGDyK)
64Cu-PCB-TE2A-Bn-NCS-c(RGDyK)
64Cu-ECB-TE2A-c(RGDyK)
64Cu-PCB-TE2A-c(RGDyK)
Blood
Liver
Kidney

Figure 4.

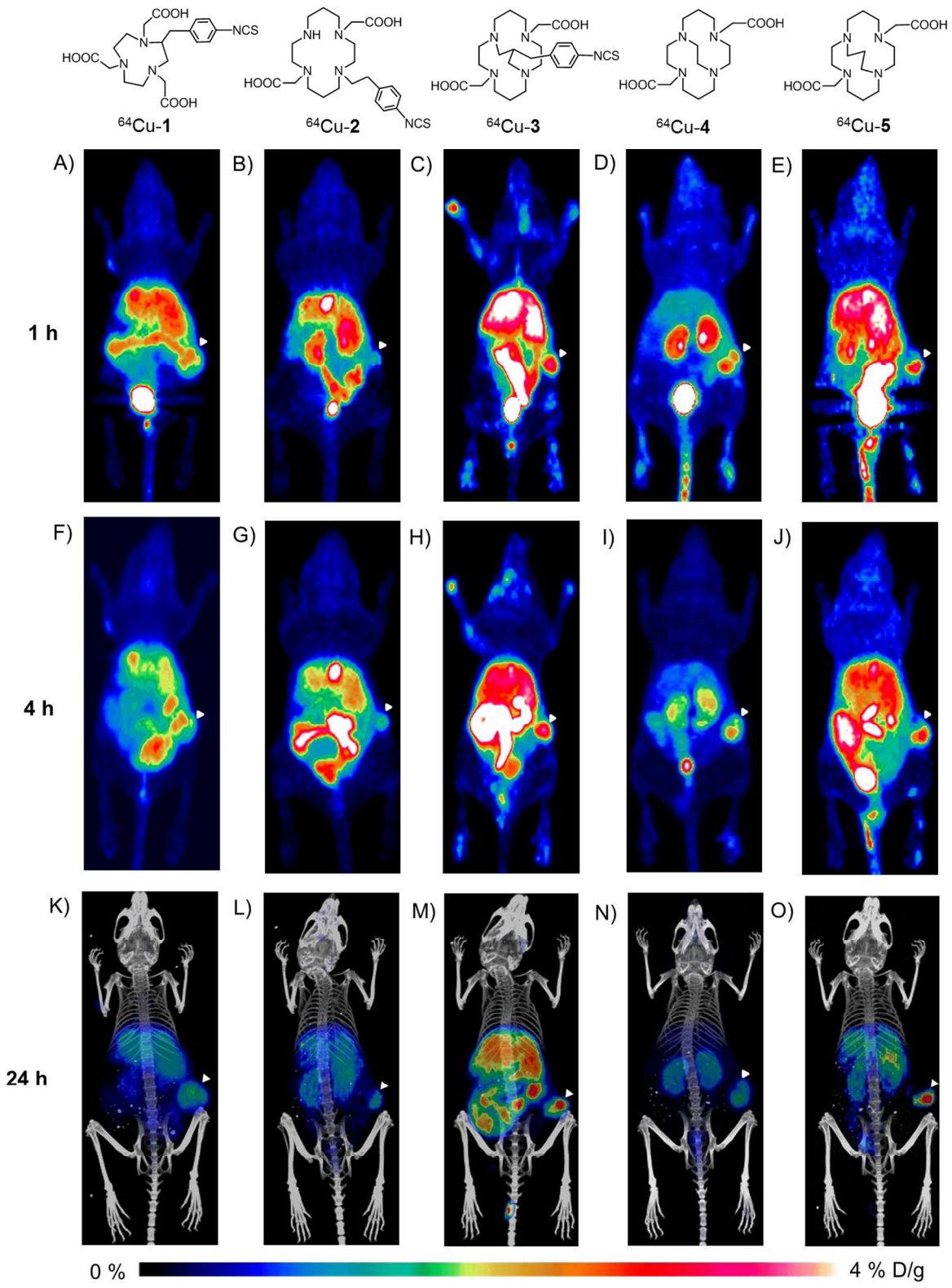
64Cu-1
64Cu-2
64Cu-3
64Cu-4
64Cu-5
A)
B)
C)
D)
E)
1 h
F)
G)
H)
I)
J)
4 h
K)
L)
M)
N)
O)
24 h
0 %
4 % D/g

Figure 5.

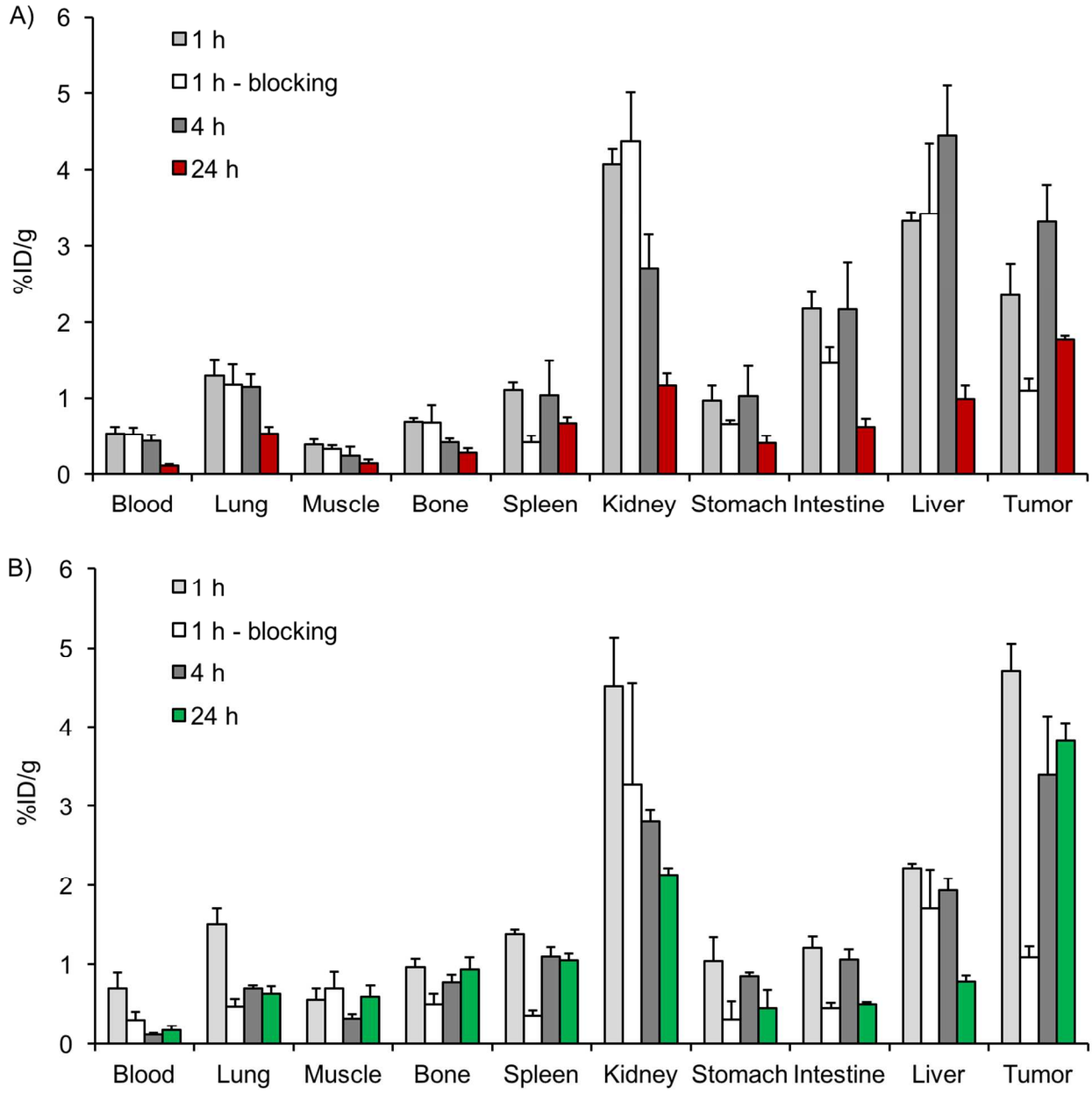
A)
%ID/g
1 h
1 h - blocking
4 h
24 h
0
1
2
3
4
5
6
Blood
Lung
Muscle
Bone
Spleen
Kidney
Stomach
Intestine
Liver
Tumor
B)
%ID/g
1 h
1 h - blocking
4 h
24 h
0
1
2
3
4
5
6
Blood
Lung
Muscle
Bone
Spleen
Kidney
Stomach
Intestine
Liver
Tumor

Figure 6.

Table 1.

A)

Bioconjugates	Organ uptake (% ID/g), 1 h				Tumor-to-organ ratio		
	Tumor (T)	Liver (L)	Kidney (K)	Muscle (M)	T/L	T/K	T/M
^{64}Cu-NOTA-Bn-NCS-c(RGDyK)	1.90 ± 0.24	2.49 ± 0.11	1.78 ± 0.17	0.41 ± 0.02	0.76 ± 0.11	1.07 ± 0.17	4.63 ± 0.63
^{64}Cu-TE2A-Bn-NCS-c(RGDyK)	1.79 ± 0.33	2.56 ± 0.25	2.87 ± 0.40	0.38 ± 0.08	0.70 ± 0.15	0.62 ± 0.14	4.71 ± 1.32
^{64}Cu-PCB-TE2A-Bn-NCS-c(RGDyK)	3.76 ± 0.21	3.91 ± 0.16	3.67 ± 0.27	0.38 ± 0.01	0.96 ± 0.07	1.02 ± 0.09	9.89 ± 0.61
^{64}Cu-ECB-TE2A-c(RGDyK)	2.23 ± 0.11	1.97 ± 0.38	3.24 ± 0.48	0.32 ± 0.02	1.13 ± 0.23	0.69 ± 0.11	6.97 ± 0.55
^{64}Cu-PCB-TE2A-c(RGDyK)	3.45 ± 0.16	3.91 ± 0.22	2.97 ± 0.45	0.48 ± 0.04	0.88 ± 0.06	1.16 ± 0.18	7.18 ± 0.69

B)

Bioconjugates	Organ uptake (% ID/g), 4 h				Tumor-to-organ ratio		
	Tumor (T)	Liver (L)	Kidney (K)	Muscle (M)	T/L	T/K	T/M
^{64}Cu-NOTA-Bn-NCS-c(RGDyK)	1.99 ± 0.22	2.20 ± 0.20	1.42 ± 0.09	0.36 ± 0.01	0.90 ± 0.13	1.40 ± 0.18	5.53 ± 0.63
^{64}Cu-TE2A-Bn-NCS-c(RGDyK)	1.86 ± 0.37	2.14 ± 0.06	1.61 ± 0.33	0.29 ± 0.06	0.87 ± 0.17	1.16 ± 0.33	6.41 ± 1.84
^{64}Cu-PCB-TE2A-Bn-NCS-c(RGDyK)	3.89 ± 0.07	3.15 ± 0.57	3.31 ± 0.28	0.36 ± 0.01	1.20 ± 0.22	1.18 ± 0.10	10.81 ± 0.36
^{64}Cu-ECB-TE2A-c(RGDyK)	1.99 ± 0.21	1.66 ± 0.25	2.49 ± 0.64	0.29 ± 0.01	1.20 ± 0.22	0.80 ± 0.22	6.86 ± 0.76
^{64}Cu-PCB-TE2A-c(RGDyK)	3.10 ± 0.10	3.13 ± 0.10	2.25 ± 0.46	0.40 ± 0.05	0.99 ± 0.04	1.38 ± 0.29	7.75 ± 1.00

C)

Bioconjugates	Organ uptake (% ID/g), 24 h				Tumor-to-organ ratio		
	Tumor (T)	Liver (L)	Kidney (K)	Muscle (M)	T/L	T/K	T/M
^{64}Cu-NOTA-Bn-NCS-c(RGDyK)	1.49 ± 0.11	1.45 ± 0.12	1.19 ± 0.09	0.22 ± 0.01	1.03 ± 0.11	1.25 ± 0.13	6.77 ± 0.59
^{64}Cu-TE2A-Bn-NCS-c(RGDyK)	1.22 ± 0.15	1.00 ± 0.20	1.12 ± 0.20	0.20 ± 0.02	1.22 ± 0.29	1.09 ± 0.24	6.10 ± 0.97
^{64}Cu-PCB-TE2A-Bn-NCS-c(RGDyK)	3.49 ± 0.10	2.73 ± 0.11	1.52 ± 0.16	0.32 ± 0.01	1.28 ± 0.06	2.30 ± 0.25	10.91 ± 0.46
^{64}Cu-ECB-TE2A-c(RGDyK)	1.11 ± 0.08	0.79 ± 0.13	1.37 ± 0.27	0.18 ± 0.02	1.41 ± 0.25	0.81 ± 0.17	6.17 ± 0.82
^{64}Cu-PCB-TE2A-c(RGDyK)	2.34 ± 0.32	1.83 ± 0.10	1.60 ± 0.38	0.31 ± 0.02	1.28 ± 0.19	1.46 ± 0.40	7.55 ± 1.14

Graphical Abstract